POLISH MARITIME RESEARCH 2(82) 2014 Vol 21; pp. 58-64
10.2478/pomr-2014-0020

Bead-on-plate welding on S235JR steel by underwater local dry chamber process

Grzegorz Rogalski, Ph. D.,
Jerzy Łabanowski, Assoc. Prof.,
Dariusz Fydrych, Ph. D.,
Jacek Tomków, M. Sc.,
Gdańsk University of Technology, Poland

ABSTRACT

The article presents the results of the effect of parameters of underwater local dry chamber welding on the properties of padding welds. The effect of heat input and the type of shielding gas on the structure and hardness of welds was established. the functions for estimating the maximum hardness of the heat affected zone have been also elaborated.

Keywords: maximum hardness of the heat affected zone; welding under water; dry chamber process

INTRODUCTION

Underwater welding is most often applied to repair – maintenance work but also in joining new elements, e.g. the welding of corrosion protection (cathodes) or quay elements [1, 2]. Wet welding technique is usually applied to underwater welding [3 ÷ 11]. It is characterized by a relatively low welding cost, easiness of manipulation of welding torch, but it also has certain disadvantages. Among the most important can be numbered the following: a greater cooling down rate of welded joint, greater amount of diffusing hydrogen as well as limitation of water depth for underwater work to about 50 m. Quality level of underwater welded joints depends to a large extent on diver – welder skill, but to reach it a special training is required, and even that does not guarranty an appriopriate quality of welded joints. Dry welding techniques which make it possible to obtain joints of identical features compared with those made in air atmosphere, have been elaborated, but such methods are very expensive [12]. It is connected with the building of special working chambers coupled with main units. Implementation of a local dry chamber which combines some features of wet and dry welding, has appeared to be an alternative to the both ways of underwater welding [13 ÷ 17]. In the method in question a diver-welder is located under water and welding process is carried out within a space isolated from water by means of special permanent or moveable chambers. The most simple and cheap solution is to apply a local dry chamber directly fixed with welding torch. Cost of the methods is much lower than that of dry welding, and features of welded joints produced this way are close to these of the joints made in dry conditions [15, 16]. Fig. 1 shows the principle of underwater welding by using the method of local dry chamber.

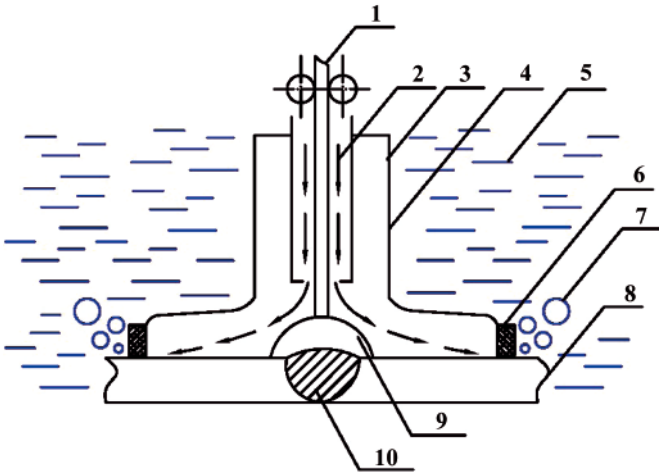

Fig. 1. *Schematic diagram of underwater welding by using the local dry chamber.* ***1)*** *wire electrode,* ***2)*** *shielding gas,* ***3)*** *inner nozzle,* ***4)*** *outer nozzle,* ***5)*** *water,* ***6)*** *flexible shield,* ***7)*** *gas bubbles,* ***8)*** *welded element,* ***9)*** *electric arc,* ***10)*** *weld [5]*

In underwater welding special attention should be paid to possible cold fracture forming. Water environment is a source of diffusing hydrogen, and short cooling down times in the temperature range of 800 ÷ 500 °C ($t_{8/5}$) contribute to the forming of hardening structures within welding joint. Therefore it is so important to be capable of predicting structures to be formed during welding. It can be realized, a. o., on the basis of hardness analysis for particular areas od welded joint. To determine influence of a type of schielding gas on hardness of padding welds is very important not only from metallurgical point of view but also for economical

reasons. The shielding gas CO_2 is cheap, and, additionally, the welding with the use of MAG (135) method in air environment is considered a low-hydrogen process, that is of a great importance in underwater conditions. Shielding gas fulfils double role during welding with the use of local dry chamber. It protects liquid metal pool and removes water from welding area.Therefore in this case shielding gas flow rate is greater than that during conventional welding process with the use of the MAG (135) method in air. It depends on a welding water depth and local chamber size. At the water depth of 1 ÷ 2 m the gas flow rate is comprised within the range of 30 ÷ 40 l/min, and at greater depths it can exceed 100 l/min. Therefore during welding at greater depths cost of shielding gas consumption can be significant.

EXPERIMENTAL TESTS

The experimental tests were aimed at determining influence of amount of heat input (welding linear energy) as well as kind of shielding gas on hardness and structure of padding welds made underwater. The tests were focused on determining analytical functions making it possible to predict maximum hardness of weld produced underwater by using the local dry chamber method.

CONDITIONS FOR REALIZATION OF EXPERIMENTAL TESTS

The tests were performed on padding welds. On the basis of literature analysis [17] it has been concluded that that differences between values of the cooling time $t_{8/5}$ for padding welds and welds made in a „V"- groove butt joint are rather low (Fig. 2). Hence it can be expected that structures obtained within padding weld area will be similar to those formed in the butt joint with butt weld.

The welding water depth was assumed on the level of 0.5 m. Water salinity was equal to the average salinity of seas and oceans (13 ‰). Amount of heat input was assumed on the level which makes it possible to produce root runs and filling ones. Values of the electric current parameters and remaining crucial variables are presented in Tab. 1.

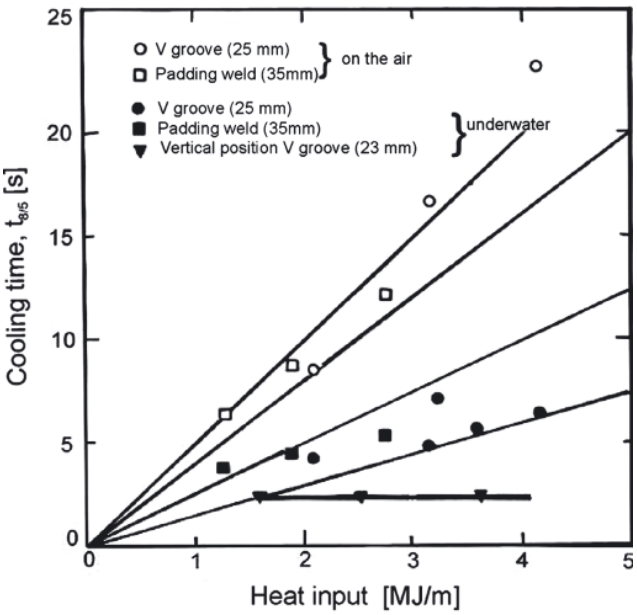

Fig. 2. *Influence of joint type on the value of cooling time $t_{8/5}$ [17]*

MATERIALS USED FOR THE TESTS

The padding welds were laid on the plates of 20 mm in thickness, made of S235JR non-alloy steel (acc. the material group 1.1 of PN CR ISO 15608 standard). The steel is characterized by a very good weldability and does not produce any troubles during welding in air. Hardness of its ferritic-pearlitic structure does not exceed 180 HV10. To produce the samples a welding wire of 2 mm diameter, marked G 38 2 C G3Si1 (acc. PN-EN ISO 14341-A), was used. Chemical composition of the steel and additional welding material is given in Tab. 2.

The welding was performed with the use of the 135 (MAG) method in atmospere of the three commonly available shielding gases:

1. CO_2, acc. PN-EN ISO 14175 – C1 (100% CO_2),
2. MIX18, acc. PN-EN ISO 14175 – M21 (18% CO_2 + + 82% Ar).
3. H5, acc. PN-EN ISO 14175 – R1 (5% H_2 + 95% Ar).

Tab. 1. *Welding parameters of samples*

Sample	Shielding gas acc. to PN-EN ISO 14175	Voltage U [V]	Welding current I [A]	Welding speed V_{sp} [m/min]	Gas flow rate W_g [l/min]	Heat input E_L [kJ/mm]
C I	C1	30	155	0.305	35	0.91
C II	C1	38	170	0.305	35	1.27
C III	C1	43	205	0.305	35	1.73
M I	M21	30.3	152	0.305	35	0.90
M II	M21	30.5	236	0.305	35	1.41
M III	M21	30.8	236	0.245	35	1.78
R I	R1	30.8	132	0.245	35	0.99
R II	R1	31.8	204	0.305	35	1.27
R III	R1	40.3	216	0.305	35	1.71

Tab. 2. *Chemical composition of materials used in the tests*

Material	Chemical composition [weight %]					
	C	Mn	Si	P	S	N
S235JR steel	0.17 ÷ 0.20	max 1.40	--	max 0.045	max 0.045	max 0.009
Welding wire G 38 2 C G3Si1	0.10	0.88	0.26	0.013	0.010	--

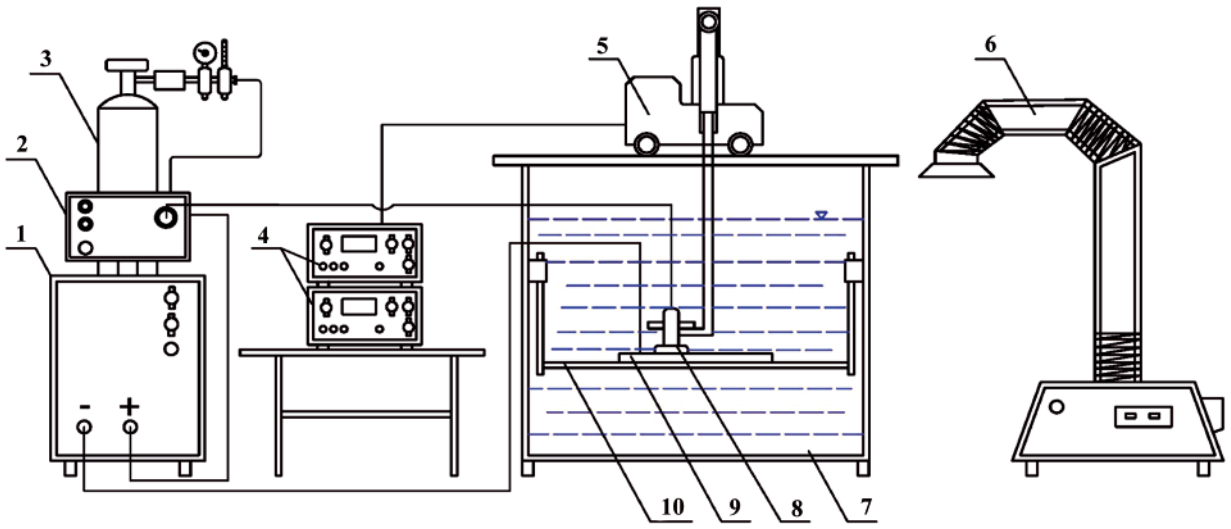

*Fig. 3. The diagram of the underwater welding at shallow depths; **1)** welding power source, **2)** wire feeder, **3)** gas cylinder, **4)** power source of trolley, **5)** welding trolley, **6)** welding fume extractor, **7)** tank, **8)** torch with the local dry chamber, **9)** plate, **10)** table*

TEST STAND FOR UNDERWATER WELDING AND CUTTING AT SHALLOW WATER DEPTHS

The padding welding was carried out on the test stand for underwater welding and cutting at shallow water depths (up to 1 m). It makes welding and padding welding in various positions as well as monitoring the processes, possible. It is equipped with ESAB ARISTO 400 welding plant (power source) which allows to record electric current parameters of the process. Component elements of the test stand are presented in Fig. 3.

RESULTS OF THE TESTS AND THEIR ANALYSIS

Hardness measurements were performed by means of Vickers (HV10) method on padding weld cross-sections. The test was carried out in compliance with PN-EN 1043-1 standard. The measurements were made in the points 2 mm distant from sample's edge, Fig. 4. The distance between imprint centres was not smaller than L=1mm. The test results are presented in Fig. 5 through 7.

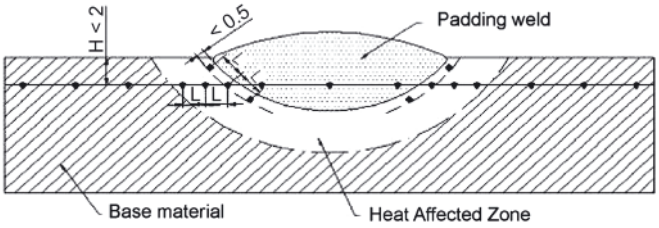

Fig. 4. Distribution of hardness on the cross - section of padding weld

When analyzing the hardness distributions over cross-sections of the padding welds in question it is observed that the greatest hardening in HAZ (abt. 400 HV10) was obtained for the samples marked MI and MII, welded in atmosphere of the shielding gas M21 (18% CO_2 + 82% Ar). Large hardness values in HAZ were also noted for the samples welded in atmosphere of the shielding gas C1 (100% CO_2), on the contrary the samples welded under the shielding gas R1 (5% H_2 + 95% Ar) do not show any large hardening in HAZ, and differences in hardness values of their padding weld material and HAZ are rather low (Tab. 3).

If the hardness recommendations contained in PN-EN ISO 15614-1standard, are taken to be an acceptance criterium (i.e.

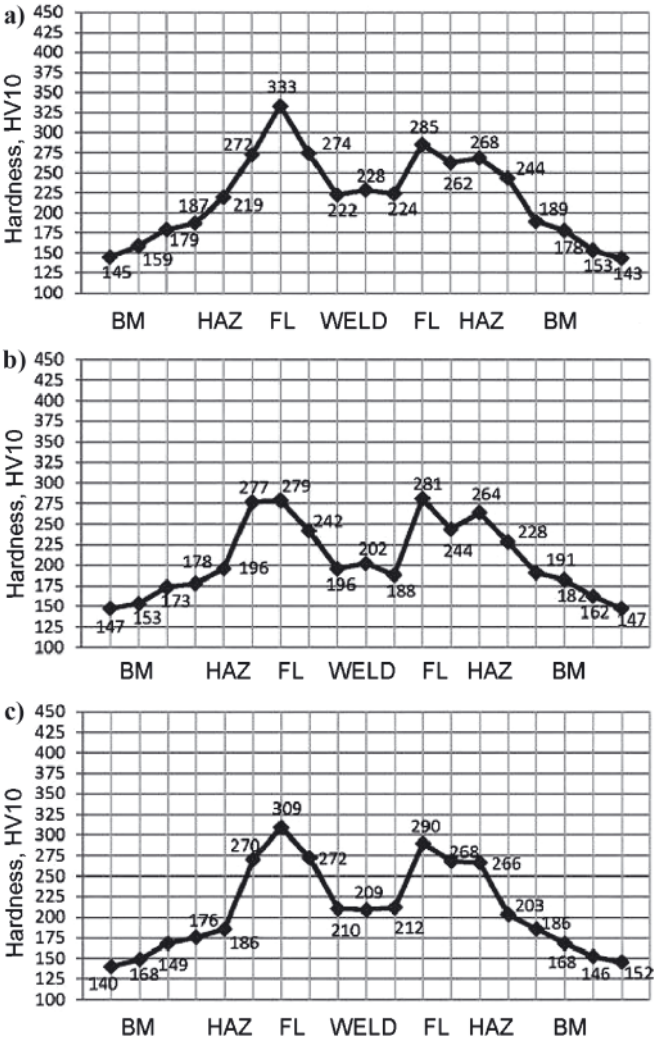

*Fig. 5. Distributions of the hardness HV10 on the cross- section of padding welds: **a)** C I, **b)** C II, **c)** C III; **BM** – base material, **HAZ** – heat affected zone, **FL** – fusion line*

380 HV10 – without heat treatment) then the samples M I and M II do not satisfy the standard's requirements (Tab. 3). The large hardness areas may show hardening structure at fusion line (for S235JR steel - bainitic structure). In underwater welding conditions it can lead to forming cold fractures.

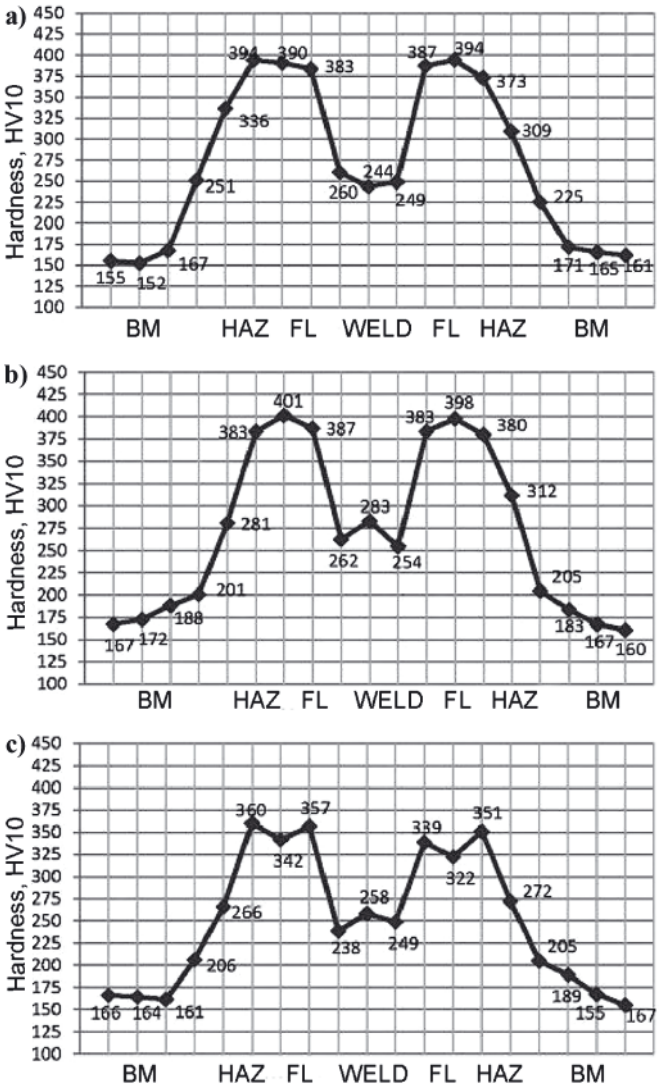

Fig. 6. Distributions of the hardness HV10 on the cross- section of padding welds: ***a)*** *M I,* ***b)*** *M II,* ***c)*** *M III*

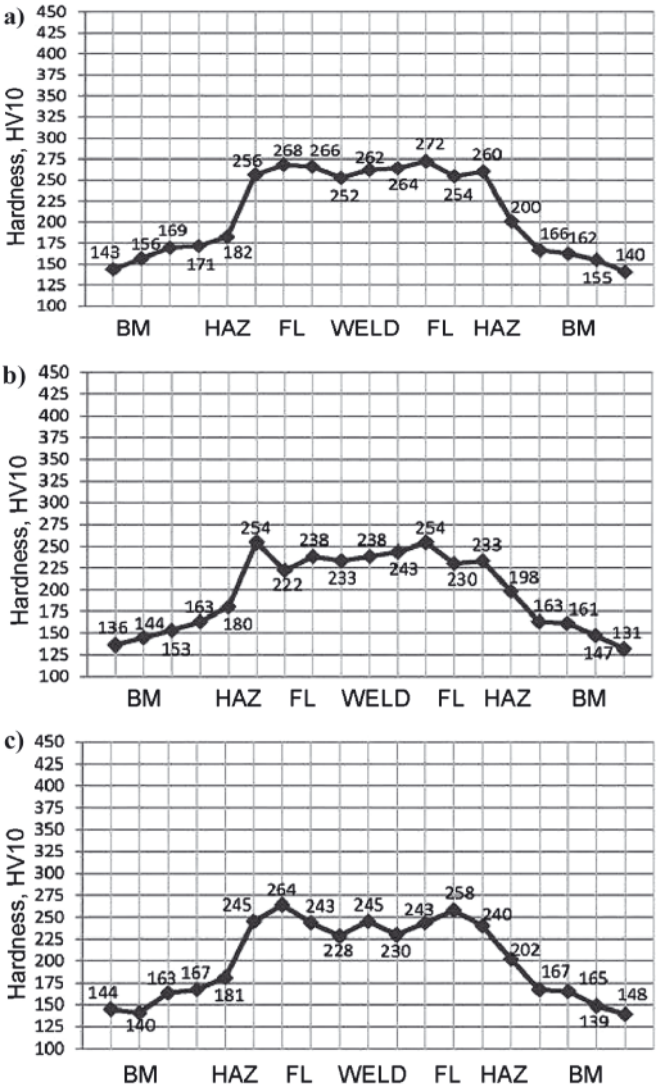

Fig. 7. Distributions of the hardness HV10 on the cross- section of padding welds: ***a)*** *R I,* ***b)*** *R II,* ***c)*** *R III*

Tab. 3. *Maximum HAZ hardness of the padding welds*

Weld	HV10 $_{max}$		
	HAZ_{left}	Weld	HAZ_{right}
C I	333	~230	285
C II	309	~210	290
C III	279	~200	281
M I	394	~250	394
M II	401	~260	398
M III	360	~250	351
R I	268	~260	272
R II	254	~240	254
R III	264	~240	258

Increase of the heat input transferred during welding within the range of 0.9 ÷ 1.7 kJ/mm, resulted in lowering maximum values of hardness in HAZ of padding welds, however no linear relation was observed. The maximum hardness values of the samples welded under the shielding gas M21 and C1 did not significantly differ from those obtained for the welding heat input of 0.9 and 1.3 kJ/mm. Only the application of the energy of abt. 1.7 kJ/mm in value resulted in HV_{max} decreasing in HAZ. For the samples prepared under the shielding gas R1 the influence of the welding heat input on the maximum hardness values in HAZ was rather slight.

It is characteristic that the padding weld metal hardness measured in the middle of weld breadth amounted to about 240 ÷ 250 HV for the samples welded under the argon - based shielding gases – M21 and R1, but the hardness of padding weld prepared under the shielding gas CO_2 (C1gas) was lower and equal to 210 ÷ 230 HV.

Application of different shielding gases affects geometry of obtained padding welds, i.e. their shape and fusion depth. Pictures of cross-sections of the obtained padding welds are presented in Fig. 8.

The increased hardness in the padding weld HAZ indicates that the building of hardening structures in this area and applied welding conditions, is possible. In order to reveal microstructures of padding welds, microscopic metallographic examinations were performed on the samples comprising padding weld cross-sections. The examinations were carried out with the use of NEOPHOT 32 optical microscope. In Fig. 9 through 11 are presented the observed microstructures of some selected samples.

The metallographic examinations demonstrated that the application of the shielding gas M21, at the welding heat input of 0.9 kJ/mm and 1.3 kJ/mm, resulted in forming the bainitic structure in HAZ, Fig. 9. In the remaining padding welds made with even lower heat input values, presence of any hardening structures in HAZ was not observed.

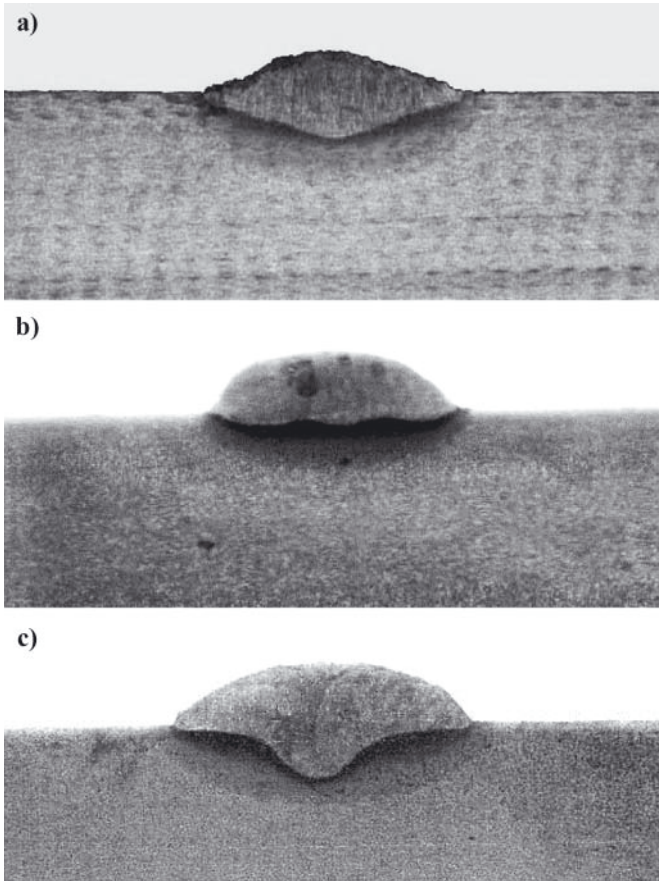

Fig. 8. *Cross-sections of padding welds:* ***a)*** *C III – C1 shielding gas,* ***b)*** *R III – R1 shielding gas,* ***c)*** *M III – M21 shielding gas*

Fig. 9. *The microstructure of M I sample (M21 shielding gas, heat input of 0.90 kJ/mm): coarse-grained structure in the HAZ, quasi-pearlite and acicular bainitic structure, visible small bands of ferrite*

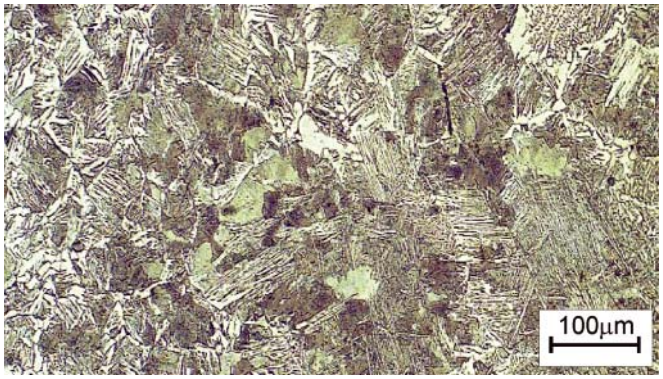

Fig. 10. *The microstructure of the R II sample (R 1 shielding gas, heat input of 1.27 kJ/mm): coarse-grained structure in the HAZ, quasi-pearlite and a small ferrite bands reaching deep into the pearlite grains forming the Widmanstätten structure*

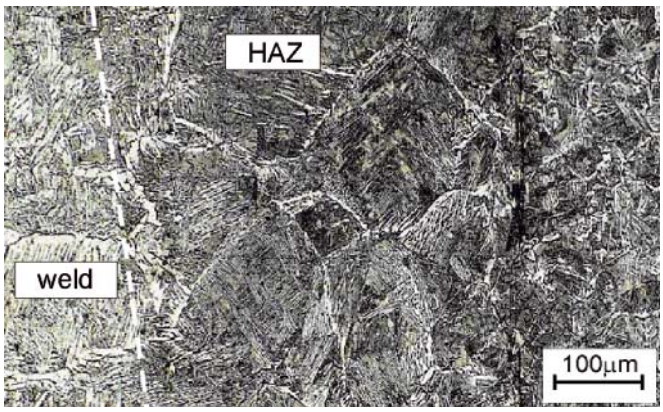

Fig. 11. *The microstructure of C I sample (C1 shielding gas, heat input of 0.91 kJ/mm): coarse-grained structure in the HAZ, quasi-pearlite surrounded by a net of ferrite, small ferrite bands reaching deep into the pearlite grains forming the Widmanstätten structure*

In conditions of underwater welding with the use of the local dry chamber method a greater rate of heat transfer from HAZ area than in air conditions, should be expected. Apart from interaction of surrounding water, intensive shielding gas flow is the other factor which affects cooling rate of the joint. The gas is applied not only to shield electric arc but also to remove all amount of water out of chamber volume. Heat transfer intensity depends not only on flow rate of the gas but also on its physical properties.

From the made observations and measurements it results that at the same welding conditions (plate thickness, immersion depth, linear energy, gas flow rate) as well as application of different shielding gases significant differences occur in maximum hardness values in HAZ of padding welds. The differences may be attributed to different values of thermal conductance coefficient of the applied shielding gases, gas influence on forming electric arc and its properties as well as chemical reactions running in high temperature of electric arc in presence of a large amount of water vapour.

The application of the mixture of argon and hydrogen (R1), a gas of a high thermal conductance, resulted in forming non-concentrated arc which produces a wide padding weld of a low fusion depth (Fig. 8b). However the high thermal conductance of hydrogen did not result in increasing cooling-down intensity of padding weld and hardness in HAZ. The application of M21 mixture composed of argon and CO_2, i.e. gases of low thermal conductance, gave a concentrated electric arc resulting in a characteristic bell form of the padding weld with deep fusion depth in the middle part (Fig. 8c). Such effect of the electric arc, at the intensive water-cooling of plate, resulted in the forming of hardening structures in HAZ and a significant rise of hardness.

Welding under the shielding gas CO_2 resulted in the forming of the so-called " hot arc" which produces a wide padding weld of a deep fusion depth (Fig. 8a). Reactions of CO dissociation and CO_2 recombination can cause phenomenon of increasing welding energy as well as burning-up alloying elements from steel to occur. To the last phenomenon can be associated decreasing the hardness in padding weld metal (Mn burning – up).

As observed, it is hard to unambiguously describe a way in which particular shielding gases affect heating and cooling intensity of HAZ of padding welds though the effects have been determined unambiguously. Moreover one should be always conscious of possible taking place of an untightness in local dry chamber and hence presence of water in welding area. Presence of water causes gas bladders close to padding weld face, and pores, to form.

The gas bladders initiate forming microfractures, which is presented in Fig. 12 and 13. Such defects lead to disqualification of a joint and its removal from operation.

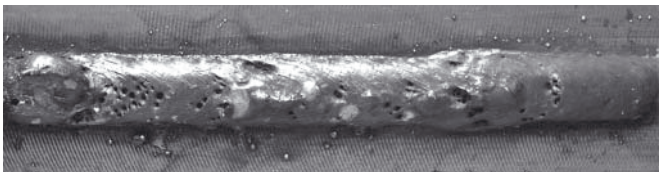

Fig. 12. *The face of the R III weld. Visible great number of pores*

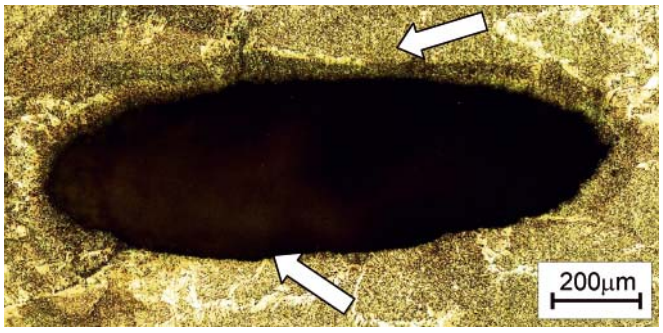

Rys. 13. *The microstructure of R III sample. Gas bladder with apparent crack initiation sites*

ELABORATION OF FORMULAE FOR DETERMINING THE MAXIMUM HARDNESS IN HAZ OF THE JOINTS

The performed tests made it possible to elaborate analytical formulae for estimating the maximum hardness in HAZ of the joints for the applied types of shielding gas as well as welding heat input values, Tab. 4. The formulae obtained from the tests, are presented in Fig. 14. As can be observed, trend lines of the diagram show an only slight decrease of hardness along with the increasing of welding heat input. This is in compliance with expectations as well as experience gained from welding in air atmosphere. However it is not possible to conclude whether it results from the effect of welding heat input itself, shielding gas type or - may be - an interaction of the both factors.

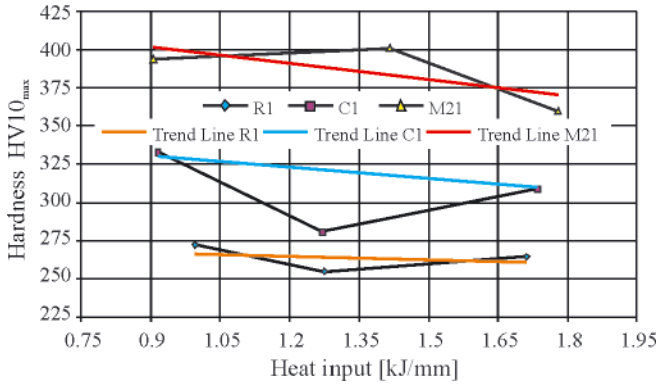

Rys. 14. *Influence of the welding heat input and type of shielding gas on HAZ maximum hardness*

Tab. 4. *The analytical functions for estimating the maximum hardness in HAZ, depending on the heat input and the type of shielding gas*

Shielding gas	Equation
M21	$HV10_{max} = -35.356 \cdot E_L + 433.41$
C1	$HV10_{max} = -25.014 \cdot E_L + 340.35$
R1	$HV10_{max} = -8.3907 \cdot E_L + 274.81$
E_L - heat input	

CONCLUSIONS

1. The maximum hardness in HAZ of the joints welded underwater with the use of the local dry chamber method depends on a type of applied shielding gas.
2. The application of the shielding gas M21 (18% CO_2 + + 82% Ar) at the amount of heat input from the range of 0.9 ÷ 1.3 kJ/mm, resulted in an excessive rise of hardness within HAZ. The observed values of the hardness reaching 400HV sugggest that a hardening structure has been formed, as confirmed by metallographic examinations.
3. The application of the shielding gas C1 (100% CO_2) as well as R1 (5% H_2 + 95% Ar) at the heat input from the range of 0.9 ÷ 1.7kJ/mm, does not cause any excessive rise of hardness within HAZ of the joints.
4. The performed investigations made it possible to elaborate the analytical formulae for determining the maximum hardness value within HAZ in case of underwater welding with the use of the local dry chamber method.
5. In order to take into account economic aspects as well as limit forming the faults like gas bladders and pores, the shielding gas C1 is recommended for underwater welding with the use of the local dry chamber method.

BIBLIOGRAPHY

1. Łabanowski J., Fydrych D., Rogalski G.: *Underwater Welding – a review*. Advances in Materials Science, 3/2008
2. Fydrych D., Łabanowski J., Rogalski G.: *Weldability of high strength steels in wet welding conditions*. Polish Maritime Research, vol. 20 (2013), no. 2, pp. 67-73
3. Matsunawa A., Nishiguchi K., Okamoto I.: *Prediction of cooling rate and hardness of base metal in the underwater welding by local cavity process.* Proceedings of the International Conference „Underwater Welding", Trondheim, Norway 1983
4. Łabanowski J., Fydrych D., Rogalski G., Samson K.: *Underwater welding of duplex stainless steel*. Diffusion and Defect Data Pt.B: Solid State Phenomena 183 (2012), pp. 101-106
5. Fydrych D., Rogalski G.: *Effect of underwater local cavity welding method conditions on diffusible hydrogen content in deposited metal*. Welding International Vol. 27 (2013), Issue 3, pp. 196-202
6. Santos V. R., Monteiro M. J., Rizzo F.C., Bracarense A. Q., Pessoa E. C. P., Marinho R. R. Vieira L. A.: *Development of an oxyrutile electrode for wet welding*. Welding Journal, vol. 91 (2012), no. 12, pp. 319-328
7. Ghadimi P., Ghassemi H., Ghassabzadeh M., Kiaei Z.: *Three-dimensional simulation of underwater welding and investigation of effective parameters*. Welding Journal, vol. 92 (2013), no. 8, pp. 239-249
8. Pessoa E., Bracarense A., Zica E., Liu S., Perez-Guerrero F.: *Porosity variation along multi-pass underwater wet welds and its influence on mechanical properties*. Journal of Materials Processing Technology. Vol. 179 (2006), Issues 1-3, pp. 239-243
9. Liu D., Zhang H., Yang K., Tang D. Feng J.: *Microstructure evolution of HAZ in the multi-pass underwater wet welded joints*. China Welding (English Edition), vol. 22 (2013), no. 1, pp. 30-34
10. Maksimov S. Y.: *Underwater arc welding of higher strength low-alloy steels*. Welding International, vol. 24 (2010), no. 6, pp. 449-454
11. Akselsen O. M., Fostervoll H., Ahlen C. H.: *Hyperbaric GMA welding of duplex stainless steel at 12 and 35 bar*. Welding Journal, vol. 88 (2009), no. 2, pp. 21-28
12. Pessoa E. C. P., Bracarense A. Q., Dos Santos V. R., Monteiro M. D. J., Vieira L. A., Marinho R. R.: *Challenges to develop an underwater wet welding electrode for "class A welds" classification, as required in the AWS D3.6 code*. ASM Proceedings of the International Conference: Trends in Welding Research 2013, pp. 259

13. Mazzaferro J. A. E., Machado I. G.: *Study of arc stability in underwater shielded metal arc welding at shallow depths*. Proceedings of the Institution of Mechanical Engineers, Part C: Journal of Mechanical Engineering Science, vol. 223 (2009), no. 3, pp. 699-710
14. Zhao B., Wu C., Jia C., Yuan X.: *Numerical analysis of the weld bead profiles in underwater wet flux-cored arc welding.* Jinshu Xuebao/Acta Metallurgica Sinica, vol. 49 (2013), no. 7, pp. 797-803
15. AleAbbas F. M., Al-Ghamdi T. A., Liu S.: *Comparison of solidification behavior between underwater wet welding and dry welding.* Proceedings of the International Conference on Offshore Mechanics and Arctic Engineering – OMAE 2011, pp. 285
16. Shi Y., Zheng Z., Huang J.: *Sensitivity model for prediction of bead geometry in underwater wet flux cored arc welding*. Transactions of Nonferrous Metals Society of China (English Edition), vol. 23 (2013), no. 7, pp. 1977-1984
17. Christensen N.: *The metallurgy of underwater welding*. Proceedings of the International Conference „Underwater Welding", Trondheim, Norway 1983

CONTACT WITH THE AUTHOR

Grzegorz Rogalski, Ph. D.,
Jerzy Łabanowski, Assoc. Prof.,
Dariusz Fydrych, Ph. D.,
Jacek Tomków, M. Sc.,
Mechanical Faculty,
Joining Engineering Department
Gdansk University of Technology
Narutowicza 11/12
80-233 Gdansk, POLAND
e-mail: jlabanow@pg.gda.pl